

TT-LSQR FOR TENSOR LEAST SQUARES PROBLEMS AND APPLICATION TO DATA MINING *

LORENZO PICCININI[†] AND VALERIA SIMONCINI[‡]

This paper is dedicated to Michela Redivo-Zaglia and Hassane Sadok

Abstract. We are interested in the numerical solution of the tensor least squares problem

$$\min_{\mathcal{X}} \|\mathcal{F} - \sum_{i=1}^{\ell} \mathcal{X} \times_1 A_1^{(i)} \times_2 A_2^{(i)} \cdots \times_d A_d^{(i)}\|_F,$$

where $\mathcal{X} \in \mathbb{R}^{m_1 \times m_2 \times \cdots \times m_d}$, $\mathcal{F} \in \mathbb{R}^{n_1 \times n_2 \times \cdots \times n_d}$ are tensors with d dimensions, and the coefficients $A_j^{(i)}$ are tall matrices of conforming dimensions. We first describe a tensor implementation of the classical LSQR method by Paige and Saunders, using the tensor-train representation as key ingredient. We also show how to incorporate sketching to lower the computational cost of dealing with the tall matrices $A_j^{(i)}$. We then use this methodology to address a problem in information retrieval, the classification of a new query document among already categorized documents, according to given keywords.

Key words. Tensor multiterm least squares, Kronecker products, rank truncation, large matrices, collocation, data mining.

AMS subject classifications. 65F45, 65F55, 15A23.

1. Introduction. We are interested in the numerical solution of the multiterm tensor least squares problem

$$(1.1) \quad \min_{\mathcal{X}} \|\mathcal{F} - \sum_{i=1}^{\ell} \mathcal{X} \times_1 A_1^{(i)} \times_2 A_2^{(i)} \cdots \times_d A_d^{(i)}\|_F,$$

where $\mathcal{X} \in \mathbb{R}^{m_1 \times m_2 \times \cdots \times m_d}$, $\mathcal{F} \in \mathbb{R}^{n_1 \times n_2 \times \cdots \times n_d}$ are tensors with d dimensions (or modes), while $A_j^{(i)} \in \mathbb{R}^{n_j \times m_j}$ are tall matrices, for $i = 1, \dots, \ell$ and $j = 1, \dots, d$. The term \mathcal{F} is assumed to be in low-rank Tucker format.

Matrix and tensor formulations of least squares problems have emerged in the recent literature as an alternative to classical vectorized forms in different data science problems, see, e.g., [5],[6],[8],[20],[16],[1]. In particular, the occurrence of a multiterm coefficient operator has been first proposed in [10],[11]. The numerical literature on the topic is very scarce, although the problem is challenging because of the absence of direct methods that can efficiently handle multiple addends in tensorial form, already for problems with small dimensions. The difficulty emerges as soon as the number of modes d is equal to three or larger, giving rise to the so-called curse of dimensionality problem. Computationally, the solution of the linear algebra problem becomes intractable. Among the strategies available in the literature, the LSQR method has been recently explored for $\ell = 1$ (one addend in (1.1)) in [2], where Tucker and CP decompositions are used.

*Version of February 4, 2025. The authors are members of the INdAM Research Group GNCS that partially supported this work.

[†]Dipartimento di Matematica, Alma Mater Studiorum - Università di Bologna, Piazza di Porta San Donato 5, 40126 Bologna, Italia. Email: lorenzo.piccinini12@unibo.it

[‡]Dipartimento di Matematica, AM², Alma Mater Studiorum - Università di Bologna, Piazza di Porta San Donato 5, 40126 Bologna, Italy, and IMATI-CNR, Via Ferrata 5/A, Pavia, Italy. Email: valeria.simoncini@unibo.it

The problem of numerically solving tensor matrix equations with *square* coefficient matrices has attracted a lot of attention in the past few decades, due to its growing occurrence in many scientific applications [15],[21],[22]. However, also in the square case, the Tucker format is hard to handle without resorting to a complete unfolding of the modes, so that direct procedures are mostly confined to low values of d ; see, e.g., [9],[37]. Except for special sparse tensor structures, see, e.g., [24], iterative methods suffer from the same memory problems.

With the classical Tucker format being too expensive, both in terms of computational costs and memory consumption, the tensor-train format (TT-format) has gained a lot of consideration, thanks to more affordable memory consumption for large d . This setting has been confirmed by our computational experience on (1.1), hence we will mainly focus on the TT-format for storing all quantities of interest, except for the coefficient matrices, which will be kept in their original form (the Kronecker product is never explicitly generated). Tensor-train formulations have been successfully used in the past decade in a variety of application problems, directly approximating the given tensor operator, or for solving linear algebra problems in tensor format; see, e.g., [31],[13], and [7] for a recent summary of contributions. The use of the TT-format is often accompanied by alternating least squares strategies, where a minimization with respect to single portions of the tensors is performed in turn. Here we take a different direction, by trying to stay as close as possible to the minimization of the whole problem, in a way that deviations are only due to the need to maintain a memory saving TT-structure.

Our contribution is twofold. First, we provide the implementation of a tensor-train version of the LSQR algorithm, a popular method introduced by Paige and Saunders in [32] for solving the large and sparse least squares problem $\min_{\mathbf{x}} \|\mathbf{f} - \mathbf{A}\mathbf{x}\|$. In the vector case, it is known that LSQR is preferable to the Conjugate Gradient (CG) on the normal equation because of stability issues, though the two methods are mathematically equivalent. Thanks to the available matlab software package TT-Toolbox [29], the tensor implementation is very natural, and the tensor-train format can be easily maintained throughout the iteration using specifically designed functions. We also propose the inclusion in our TT-LSQR method of a randomized strategy via Johnson-Lindenstrauss transforms, to lighten the computational costs when the problem becomes very large. Our second contribution is the investigation of the problem formulation (1.1) in addressing a recurrent problem in information retrieval associated with term-document data: the allocation of a new query document among groups of documents, which were already clustered using keyword terms as discriminant. Our computational experience shows that the approach is very promising and could be easily adapted to very large datasets by exploiting the features of the randomized projection.

An outline of the paper follows. In section 2 we recall some tensor properties and notation, mostly focusing on the tensor-train (TT-) format. Section 3 describes the tensor-oriented implementation of the LSQR method, while section 3.1 specializes to the TT-format. Section 4 and its subsections briefly describe the procedures we have considered to enhance the computational performance of the developed method, that is, preconditioning and randomized sketching. As a preliminary “sanity check” step, the new algorithm and its features are explored on square problems in section 5. In section 6 the problem of interest in the context of Information Retrieval is introduced. In section 7 and its subsections a large number of experiments on the allocation problem with several benchmark datasets is reported. In particular, in section 7.3 we describe how to exploit sketching strategies to make the whole procedure computa-

tionally more efficient, while the conclusions are drawn in section 8. The Appendix reports some relevant aspects associated with the Tucker format, in case that tensor formulation is of interest.

2. Preliminaries. A tensor is a multidimensional array $\mathcal{A} \in \mathbb{R}^{n_1 \times \dots \times n_d}$, denoted by capital italic letters to distinguish them from matrices. The tensor is said to be d -dimensional if it has d dimensions (or *modes*). One important operation with tensors is the so-called j -mode product: given a tensor $\mathcal{A} \in \mathbb{R}^{n_1 \times \dots \times n_d}$ and a matrix $U \in \mathbb{R}^{m \times n_j}$, the j -mode product is denoted by

$$\mathcal{B} = \mathcal{A} \times_j U \in \mathbb{R}^{n_1 \times \dots \times m \times \dots \times n_d},$$

defined as follow

$$\mathcal{B}(i_1, \dots, i_{j-1}, k, i_{j+1}, \dots, i_d) = \sum_{i_n=1}^{n_j} \mathcal{A}(i_1, \dots, i_j, \dots, i_d) U(k, i_j).$$

The properties of the j -mode product are described in [23]. We recall the correspondence between the j -mode products and the Kronecker products. Given a tensor $\mathcal{X} \in \mathbb{R}^{n_1 \times \dots \times n_d}$ and the matrices $A^{(j)} \in \mathbb{R}^{m_j \times n_j}$, $j = 1, \dots, d$, we have

$$\mathcal{Y} = \mathcal{X} \times_1 A^{(1)} \times_2 A^{(2)} \dots \times_d A^{(d)} \quad \Leftrightarrow \quad \mathbf{y} = (A^{(d)} \otimes \dots \otimes A^{(1)}) \mathbf{x},$$

where \mathbf{y} and \mathbf{x} denote the vectorization of the tensors \mathcal{Y} and \mathcal{X} , respectively.

Given the introduction of the n -mode product, the Tucker decomposition is a natural associated tensor factorization.

DEFINITION 2.1. *Given a tensor $\mathcal{X} \in \mathbb{R}^{n_1 \times \dots \times n_d}$, the Tucker decomposition of \mathcal{X} is defined as*

$$\mathcal{X} \approx \mathcal{C} \times_1 A^{(1)} \times_2 A^{(2)} \dots \times_N A^{(d)},$$

where $\mathcal{C} \in \mathbb{R}^{m_1 \times \dots \times m_d}$ is the core tensor and $A^{(j)} \in \mathbb{R}^{n_j \times m_j}$.

If the matrices $A^{(i)}$ of the Tucker decomposition are full column rank, the decomposition is said to be *independent*; if the matrices $A^{(i)}$ have orthonormal columns, the decomposition is said to be *orthonormal*. In Figure 2.1 an example of Tucker decomposition of a 3-dimensional tensor is shown.

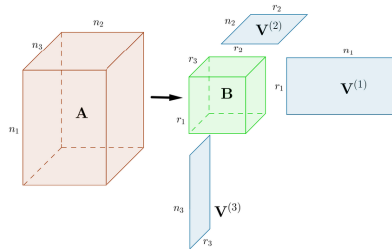


FIG. 2.1. Tucker format.

Alternatively, a very popular tensor representation is the Tensor-Train (TT) decomposition. A tensor \mathcal{X} is in TT-format if

$$(2.1) \quad \mathcal{X}(i_1, i_2, \dots, i_d) = G_1(i_1, :) G_2(:, i_2, :) \dots G_d(:, i_d),$$

where each $G_k(:, i_k, :) \in \mathbb{R}^{r_{k-1} \times r_k}$, under the assumption $r_0 = r_d = 1$.

We can interpret each $G_k(:, i_k, :)$ as a matrix, and the whole of G_k as a three-dimensional tensor, with dimensions $r_{k-1} \times n_k \times r_k$. Consequently, each element of \mathcal{X} can be seen as

$$\begin{aligned} \mathcal{X}(i_1, i_2, \dots, i_d) &= \sum_{\alpha_0, \alpha_1, \dots, \alpha_d} G_1(\alpha_0, i_1, \alpha_1) G_2(\alpha_1, i_2, \alpha_2) \cdots G_d(\alpha_{d-1}, i_d, \alpha_d) \\ (2.2) \quad &= \sum_{\alpha_1, \dots, \alpha_{d-1}} G_1(i_1, \alpha_1) G_2(\alpha_1, i_2, \alpha_2) \cdots G_d(\alpha_{d-1}, i_d). \end{aligned}$$

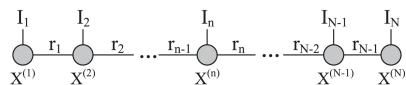


FIG. 2.2. *Tensor-Train format.*

In the Tensor-Train format, a tensor is low-rank if each TT-rank is small, $r_i \ll n_i$. Classically, low rank is obtained through the *rounding* operation, based on the (truncated) TT-SVD algorithm, introduced by Oseledets in [28]. Therefore, rounding has the role of what we call truncation function for other formats. We refer to section 3.1 for a few more details on the TT-SVD.

3. Truncated Tensor-Oriented LSQR. In this section, we introduce the numerical method for solving the tensor least squares problem (1.1).

A straightforward way to solve (1.1), under the assumption $m = m_1 = \dots = m_d$, employs vectorization through the Kronecker product, that is

$$\mathbf{A} = \sum_{i=1}^{\ell} A_d^{(i)} \otimes A_{d-1}^{(i)} \otimes \dots \otimes A_1^{(i)} \in \mathbb{R}^{(n_1 n_2 \cdots n_d) \times m^d}, \quad \mathbf{f} = \text{vec}(\mathcal{F}) \in \mathbb{R}^{n_1 n_2 \cdots n_d}$$

and $\mathbf{x} = \text{vec}(\mathcal{X}) \in \mathbb{R}^{m^d}$, and solves the vectorized least squares problem with classical iterative LS methods. This procedure is inefficient due to the final dimensions of \mathbf{A} , which become infeasible even for a small initial problem size. Nonetheless, the Kronecker formulation is useful to analyze the spectral properties of the problem.

For $d = 2$ the problem is reduced to a matrix least squares problem. For $\ell = 2$ a truncated matrix-oriented LSQR algorithm has been recently studied in [34], where the implementation and properties of the truncated matrix-oriented LSQR are introduced to solve the generalized Sylvester least squares problem

$$(3.1) \quad \min_{X \in \mathbb{R}^{m \times m}} \|F_1 F_2^T - A_1^{(1)} X A_2^{(1)} - A_1^{(2)} X A_2^{(2)}\|_F,$$

with $A_1^{(j)}, (A_2^{(j)})^T \in \mathbb{R}^{n \times m}$ and $F_1, F_2 \in \mathbb{R}^{n \times p}$, $p \ll \min\{n, m\}$. The method in [34] is equipped with a computational efficient strategy to generate updated iterates of low rank. Because of better numerical properties and a more efficient truncation function, truncated LSQR outperforms truncated CG on the normal equation, when solving matrix least squares problems.

We derive the truncated tensor-oriented LSQR keeping in mind the matrix-oriented procedure, although it is immediately clear that the level of complexity is much higher. The first step substitutes vectors with tensors,

$$\mathbf{x}^{(k+1)} = \mathbf{x}^{(k)} + \frac{\phi_{k+1}}{\rho_{k+1}} \mathbf{d}^{(k+1)} \implies \mathcal{X}^{(k+1)} = \mathcal{X}^{(k)} + \frac{\phi_{k+1}}{\rho_{k+1}} \mathcal{D}^{(k+1)}.$$

With this preliminary step, the computed iterates are the same as those obtained in the vectorization case, but formally reshaped as tensors. In fact, after the sum above the updated tensor needs to preserve the structure, while keeping memory requirements under control by ensuring that the rank remains small. Since a sum generally increases the rank, some truncation is necessary, like in the matrix case. To adapt the aforementioned truncation strategy to the tensor case, it is necessary to take into account the tensor formats being used. We will mainly focus on the Tensor-Train (TT) format introduced in Section 2, keeping in mind that the Tucker format has a different strategy for maintaining the low-rank tensor format of sums of tensors. Summarizing, every time a tensor update is performed the sum requires to be computed within the chosen format, and then truncation is applied, again following the format characterization. The same occurs when the coefficient operator and its transpose is applied.

Preliminary computational experiments showed that the Tucker formulation is far from being competitive for the class of data we are interested in, both in terms of memory requirements and computational costs, already with $d = 3$ modes; this fact has been largely observed in the recent literature. For this reason, in the following we focus on the description of the tensor-train properties, while the discussion of the Tucker format is included for completeness in the Appendix.

Algorithm 3.1 TT-LSQR ALGORITHM

Require: $A_j^{(i)}$ with $j = 1, \dots, d$ and $i = 1, \dots, \ell$, \mathcal{F} , imax
 $\beta_1 \mathcal{U}_1 = \mathcal{F}$, $\alpha_1 \mathcal{V}_1 = \mathcal{L}^T(\mathcal{U}_1)$, $\mathcal{G}_1 = \mathcal{V}_1$, $\mathcal{X}_0 = \iota$, $\bar{\Phi}_1 = \beta_1$, $\bar{\rho}_1 = \alpha_1$
while $i < \text{imax}$ **do**
 $i = i + 1$
 $\beta_{i+1} \mathcal{U}_{i+1} = \mathcal{L}(\mathcal{V}_i) - \alpha_i \mathcal{U}_i$
 $\alpha_{i+1} \mathcal{V}_{i+1} = \mathcal{L}^T(\mathcal{U}_{i+1}) - \beta_{i+1} \mathcal{V}_i$
 $\rho_i = (\bar{\rho}_i^2 + \beta_{i+1}^2)^{1/2}$
 $c_i = \bar{\rho}_i / \rho_i$, $s_i = \beta_{i+1} / \rho_i$
 $\theta_{i+1} = s_i \alpha_{i+1}$, $\bar{\rho}_{i+1} = -c_i \alpha_{i+1}$
 $\Phi_i = c_i \bar{\Phi}_i$, $\bar{\Phi}_{i+1} = s_i \bar{\Phi}_i$
 $\mathcal{X}_i = \mathcal{X}_{i-1} + (\Phi_i / \rho_i) \mathcal{G}_i$
 $\mathcal{G}_{i+1} = \mathcal{V}_{i+1} - (\theta_{i+1} / \rho_i) \mathcal{G}_i$
 test for convergence
end while

3.1. Tensor-train LSQR. The implementation of tensor-oriented LSQR in tensor train format, TT-LSQR in the sequel, is presented in Algorithm 3.1. In there, calligraphic Roman letters refer to tensors, while Greek letters refer to scalars (as an exception, c_i, s_i also refer to scalars). The operations have to be adapted to the tensor setting: section 3.1 discusses the tensor-train format, while the appendix reports the Tucker format. Here we just anticipate that thanks to particularly advanced software packages for tensor computations, the actual implementation does not substantially differ from Algorithm 3.1, since all elementary operations involving tensors are overwritten, and thus carried out according to their format¹. Moreover, extra truncation can be applied, called “rounding” in the tensor-train format, to reduce the inner

¹The code associated with Algorithm 3.1 will be made available in <https://github.com/Lorenzo-Piccinini/> in the near future.

tensors size. We will return to this issue later in this section.

In the TT-format the concept of low-rank TT-tensor is inherent in the format itself. Theoretical results to estimate the error occurring when operating in the TT-format are available. In particular, if we assume that the given tensor is only approximately low-rank, i.e. the unfoldings satisfy

$$(3.2) \quad A_k = R_k + E_k, \quad \text{rank}(R_k) = r_k, \quad \|E_k\|_F = \epsilon_k, \quad k = 1, \dots, d-1,$$

then the error can be estimated as follows.

THEOREM 3.1. ([30]). *Suppose that the unfoldings A_k of the tensor \mathcal{A} satisfy (3.2). The TT-SVD computes a tensor \mathcal{B} in the TT-format with TT-ranks r_k and*

$$(3.3) \quad \|\mathcal{A} - \mathcal{B}\|_F^2 \leq \sum_{k=1}^{d-1} \epsilon_k^2,$$

where ϵ_k is the distance (in the Frobenius norm) from A_k to its best rank- r_k approximation

$$\epsilon_k = \min_{\text{rank}(B) \leq r_k} \|A_k - B\|_F.$$

Usually, an SVD adapted to the TT context is used to approximate a full tensor with another one in TT-format (see below). In our case, the tensors are given in TT-format, but with sub-optimal TT-ranks due to the addition, which means that the tensor can be represented by another TT-tensor having lower TT-ranks. The TT-SVD algorithm can be adapted to these purposes. The complexity in this case is greatly reduced, while the error estimate does not change [28]. The procedure takes the name of what we have already called *rounding*.

The considerations above are necessary to appreciate how operations such as sums and products are affected by rounding inside the LSQR algorithm. Indeed, whenever two TT-tensors $\mathcal{A}, \mathcal{B} \in \mathbb{R}^{n_1 \times \dots \times n_d}$ are added, the resulting tensor will have cores defined as

$$C_1(i_1) = [A_1(i_1) \quad B_1(i_1)], \quad C_d(i_d) = \begin{bmatrix} A_d(i_d) \\ B_d(i_d) \end{bmatrix},$$

and

$$C_k(i_k) = \begin{bmatrix} A_k(i_k) & 0 \\ 0 & B_k(i_k) \end{bmatrix}, \quad k = 2, \dots, d-1.$$

The sum tensor $\mathcal{C} = \mathcal{A} + \mathcal{B}$ belongs to $\mathbb{R}^{n_1 \times \dots \times n_d}$ and, if r_i^A and r_i^B are the TT-ranks of \mathcal{A} and \mathcal{B} respectively, the TT-ranks of \mathcal{C} are $r_i^C = r_i^A + r_i^B$. Hence, whenever two or more tensors are added, the TT-ranks increase, and rounding becomes necessary to control the ranks. These truncations are taken care of in the Tensor-Train package [29], by using a tensor-train SVD. This TT-SVD algorithm ([28]) is presented as an algorithm to compute the TT decomposition of a given tensor \mathcal{A} . If the tensor is already in TT-format, its complexity is reduced. In particular, given a tensor $\mathcal{A} \in \mathbb{R}^{n_1 \times \dots \times n_d}$ with suboptimal TT-ranks r_k , we want to estimate the reduced ranks \bar{r}_k given an accuracy ϵ to preserve. We follow the description in [28]: Recalling that

$$\mathcal{A}(i_1, i_2, \dots, i_d) = G_1(i_1)G_2(i_2) \cdots G_d(i_d),$$

we first proceed with a Right-to-Left orthogonalization of the cores, and then compress the TT-ranks through the SVD decomposition. To simplify the description, let us consider a 3-dimensional tensor $G \in \mathbb{R}^{r_{k-1} \times n_k \times r_k}$, indexed as $G(\alpha_{k-1}, i_k, \alpha_k)$. The matrix $G(\alpha_{k-1}, i_k, \alpha_k)$ denotes its unfolding of dimensions $r_{k-1} \times n_k r_k$ and $G(\alpha_{k-1} i_k, \alpha_k)$

its unfolding of dimensions $r_{k-1}n_k \times r_k$. Starting from the d th core up to the 2nd core, at the k th iteration we compute the QR decomposition of the k th core $G_k \in \mathbb{R}^{r_{k-1} \times n_k \times r_k}$

$$[G_k(\beta_{k-1}, i_k \beta_k), R_k(\alpha_{k-1}, \beta_{k-1})] = \text{QR}_{\text{rows}}(G_k(\alpha_{k-1}, i_k \beta_k)),$$

such that

$$G_k(\alpha_{k-1}, i_k \beta_k) = R(\alpha_{k-1}, \beta_{k-1})G_k(\beta_{k-1}, i_k \beta_k),$$

where QR_{rows} denotes the reduced QR decomposition applied to the transpose of a matrix, leading to $G_k \in \mathbb{R}^{r_{k-1} \times n_k \times r_k}$ and $R_k \in \mathbb{R}^{r_{k-1} \times r_{k-1}}$. The $(k-1)$ th TT-core is then updated as $G_{k-1} = G_{k-1} \times_3 R_k$.

The second step consists of the compression of the computed cores. Starting from the 1st core up to the $(d-1)$ th core, at the k th iteration the core G_k is reduced via a singular value decomposition, that is $[G_k(\beta_{k-1} i_k, \gamma_k), \Lambda_k, V_k(\beta_k, \gamma_k)] = \text{SVD}(G_k(\beta_{k-1} i_k, \beta_k))$, where $G_k(\beta_{k-1} i_k, \gamma_k) \in \mathbb{R}^{\bar{r}_{k-1} n_k \times \bar{r}_k}$, $V_k(\beta_k, \gamma_k) \in \mathbb{R}^{r_k \times \bar{r}_k}$, $\bar{r}_k < r_k$ and $\Lambda_k \in \mathbb{R}^{\bar{r}_k \times \bar{r}_k}$. Then the next core is updated as $G_{k+1} = G_{k+1} \times_1 (V_k \Lambda_k)^T$.

At the end of the TT-SVD algorithm the new TT-cores have dimension $\bar{r}_{k-1} \times n_k \times \bar{r}_k$, where \bar{r}_k are the ranks obtained from the reduced SVD. Further details can be found in [28].

4. Computational devices to improve performance. The vector LSQR algorithm may show slow convergence, when the normal equation has an ill-conditioned coefficient matrix. Computational devices such as preconditioning have been proposed to enhance the method performance. In the following section we recall how to extend the preconditioning strategy to our structured coefficient matrix. To lower the computational costs of the whole procedure, in section 4.2 we also consider recently developed sketching strategies, which seem to adapt well to the sum of Kronecker operators.

4.1. Preconditioning for Tensor-oriented LSQR. The use of tensors makes each LSQR iteration significantly expensive, and the cost increases at each iteration until the maximum rank threshold is reached. After that the cost per iteration remains approximately constant, though high, until termination is reached. To limit computational costs we can apply preconditioning, so as to decrease the total number of iterations performed.

For the least squares problem, we consider right preconditioning [3],[17]. Given a least squares problem,

$$\min_{\mathbf{x}} \|\mathbf{f} - \mathbf{A}\mathbf{x}\|,$$

with $\mathbf{A} \in \mathbb{R}^{n \times m}$, $\mathbf{x} \in \mathbb{R}^m$ and $\mathbf{f} \in \mathbb{R}^n$, we look for a matrix $\mathbf{M} \in \mathbb{R}^{m \times m}$ called *preconditioner* such that the matrix $\mathbf{A}\mathbf{M}^{-1}$ satisfies $\kappa(\mathbf{A}\mathbf{M}^{-1}) \leq \kappa(\mathbf{A})$, where $\kappa(\cdot)$ denotes the condition number. The problem is transformed as follows,

$$\min_{\mathbf{y}} \|\mathbf{f} - \mathbf{A}\mathbf{M}^{-1}\mathbf{y}\|, \quad \mathbf{y}^* = \mathbf{M}\mathbf{x}^*.$$

The final solution is recovered as $\mathbf{x}^* = \mathbf{M}^{-1}\mathbf{y}^*$. The matrix \mathbf{M} is chosen in such a way that solving linear systems with \mathbf{M} is sufficiently cheap.

In our tensor least squares problem the matrix \mathbf{A} is replaced by the tensor $\mathcal{A} = \sum_{i=1}^{\ell} \mathcal{A}^{(i)} = \sum_{i=1}^{\ell} A_d^{(i)} \otimes A_{d-1}^{(i)} \otimes \dots \otimes A_1^{(i)}$, $\mathbf{x} = \text{vec}(\mathcal{X})$ and $\mathbf{f} = \text{vec}(\mathcal{F})$. Depending on the problem, the single term $A_j^{(i)}$ may have few columns. Therefore, it is convenient

to choose as \mathbf{M} the upper triangular factor of the QR decomposition of selected coefficient matrices $\mathbf{A}^{(i)} = \mathbf{Q}^{(i)} \mathbf{R}^{(i)}$, that is

$$\mathbf{A}_j^{(i)} = \mathbf{Q}_j^{(i)} \mathbf{R}_j^{(i)} \implies \mathbf{R}^{(i)} = \mathbf{R}_d^{(i)} \otimes \mathbf{R}_{d-1}^{(i)} \otimes \cdots \otimes \mathbf{R}_1^{(i)}.$$

In practice, for a fixed mode, we compute the upper triangular factor for all $i = 1, \dots, \ell$, and for each mode $j = 1, \dots, d$ we choose the $\mathbf{R}_j^{(i)}$ with the lowest condition number. The preconditioner will be

$$\mathbf{M} = \mathbf{R}_d^{(i_d)} \otimes \mathbf{R}_{d-1}^{(i_{d-1})} \otimes \cdots \otimes \mathbf{R}_1^{(i_1)},$$

where $i_j = \arg \min_{i=1, \dots, \ell} \kappa(\mathbf{R}_j^{(i)})$. The strategy takes into account the fact that all matrices for each mode have similar data, so that $\mathbf{R}_j^{(i_j)}$ may be effective on all matrices of the j th mode.

If the data are sparse, the preconditioned matrices $\mathcal{A}^{(i)} \mathbf{M}^{-1}$ do not need to be explicitly built. On the other hand, if the number of dense columns of $\mathcal{A}^{(i)}$ is small, the preconditioned matrices are worth being computed once for all before starting the procedure.

4.2. Sketching for performance. Although the use of tensors allows us to save memory, the matlab implementation of TT-LSQR yields unsatisfactory CPU time performance. Rank truncation alleviates this problem, however speed remains an important bottleneck. We addressed this issue by using randomized linear algebra to solve overdetermined least squares problems [35]. More precisely, we introduce an operator $\mathcal{S} : \mathbb{R}^n \rightarrow \mathbb{R}^s$ with $s = 2d\bar{m}$, where d is the number of modes in coefficient operator, and \bar{m} is the total number of columns in each mode; hence, s is twice the overall number of data columns involved in the computation. The operator \mathcal{S} acts as a projection onto a vector subspace of \mathbb{R}^s , significantly reducing the dimensions. This corresponds to replacing the problem $\min_{\mathbf{x}} \|\mathbf{f} - \mathcal{A}\mathbf{x}\|$ with $\min_{\mathbf{x}} \|\mathcal{S}(\mathbf{f} - \mathcal{A}\mathbf{x})\|$.

For the definition of \mathcal{S} we consider the popular Johnson-Lindenstrauss transform, giving rise to the so-called sketching operator ([38],[26]). This transform is given by the composition of a diagonal matrix D of ± 1 with probability $1/2$, then a Hadamard or Fourier-type transform H , and then a row sampling operator J , giving $\mathcal{S}(A) = \frac{1}{\sqrt{m\bar{n}}} JHDA$.

Letting \mathbf{x}_0 be the solution to the sketched problem, it can be shown [26] that for a fixed $\epsilon > 0$, bounds of the type

$$\|\mathbf{f} - \mathcal{A}\mathbf{x}_0\| \leq \frac{1+\epsilon}{1-\epsilon} \min_{\mathbf{x}} \|\mathbf{f} - \mathcal{A}\mathbf{x}\|. \quad \text{for } s \sim n \log n / \epsilon^2.$$

For our setting, the procedure corresponds to projecting the space of keywords (for the term-document datasets) or the space of pixels (for the image dataset) into a significantly smaller vector subspace. We construct a single sketching operator \mathcal{S} that acts on the matrix of each mode, for all terms, and we apply the operator so that the coefficient matrices become $\widehat{A}_j^{(i)} = \mathcal{S}(A_j^{(i)})$. The reduced problem to be solved thus reads as follows

$$(4.1) \quad \min_{\mathbf{x}} \|\mathcal{S}(\mathbf{f}) - \left(\sum_{i=1}^{\ell} \widehat{A}_d^{(i)} \otimes \cdots \otimes \widehat{A}_1^{(i)} \right) \mathbf{x}\|.$$

Thanks to the choice $s \ll n$, the solution of (4.1) significantly reduces the computational cost of the classification. In section 7.3 we report on our computational experience with this strategy.

5. Computational experiments with discretized PDEs. In this section we present a preliminary experimental analysis of the Truncated Tensor LSQR with Tensor-Train format.

We consider the discretization by centered finite differences of the partial differential equation

$$-\Delta u + 2 \exp(1-x)u_x = f, \quad u = u(x, y, z), \quad (x, y, z) \in [0, 1]^3,$$

equipped with uniform Dirichlet boundary conditions. Here f is constant and equal to 1. Upon discretization, the problem can be written as

$$(5.1) \quad (T \otimes I \otimes I + I \otimes T \otimes I + I \otimes I \otimes (T + B)) \mathbf{x} = \mathbf{f},$$

where $T \in \mathbb{R}^{n \times n}$ is the usual tridiagonal matrix corresponding to the one-dimensional approximation of the negative second order derivative, and $B \in \mathbb{R}^{n \times n}$ is the centered finite difference approximation of $2 \exp(1-x)u_x$. We use this square problem as a “sanity check” test, since the linear equation itself would not require a method for least squares problems to be solved. The fact that the equation residual goes to zero allows us to easily focus on different features of the method, such as the dependence on the truncation parameters.

In the left plot of Figure 5.1 we report the convergence history of our new method applied to (5.1) for $n = 50$, as the TT truncation parameter varies. As expected, stagnation occurs at a level that is related to the employed threshold. The results are in full agreement with what happens in the matrix case when the truncation threshold increases, see, e.g., [25] for similar results using CG for symmetric and positive definite problems. The right plot of Figure 5.1 shows the convergence behavior of the method with truncation threshold 10^{-9} , as the maximum allowed rank of the TT-cores varies. Convergence is similarly affected. In general, truncation of information may be severe when applying the operator \mathcal{L} with several terms, that is for ℓm large. Indeed, the TT-cores resulting after multiplications by \mathcal{L} have size up to ℓ times the size of the argument tensor. For this problem, the maximum rank equal to n appears to be sufficient, and this is related to the fact that for this problem there is a single non-identity matrix for each mode, hence each TT-core behaves as if $\ell = 1$.

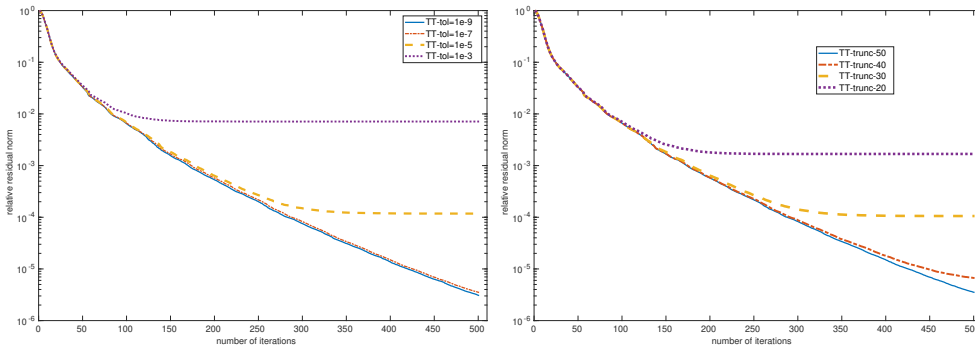


FIG. 5.1. Convergence history of TT-LSQR for $n = 50$ for problem (5.1). Left: Behavior as the TT truncation threshold varies. Right: Behavior as the TT truncation rank varies (truncation threshold 10^{-8}).

The second experiment stems from the finite difference discretization of a modi-

fication of the previous problem, that is

$$(5.2) \quad (a(x)u_x)_x + (a(y)u_y)_y + (a(z)u_z)_z + u_x = f,$$

while the other settings are unchanged. Here $a(x) = -\exp(-x)$, for $x \in (0, 1)$, so that the discretization of each second order derivative evaluates $a(x)$ at the midpoint of each discretization subinterval. The tensor equation takes again the form (5.1), where however T and B have different meanings. With this experiment we are interested in comparing the performance of TT-LSQR with that of the matrix version of the problem, which we call MATRIX-LSQR; for the latter we use the matrix LSQR method developed in [34]. The matrix-oriented formulation of the problem can be obtained by collecting one of the Kronecker products, giving

$$(5.3) \quad TX + X(T \otimes I + I \otimes (T + B))^T = \mathbf{f}_1 \mathbf{f}_2^T,$$

with clear meaning for $\mathbf{f}_1, \mathbf{f}_2$; see, e.g., [33]. Note that X is a rectangular matrix of size $n_3 \times n_2 n_1$. Given the structure of the problem, in the matrix case truncation acts differently than in the tensor case: all iterates have factors with either n_1 rows or $n_2 n_3$ columns each, hence memory requirements grow more significantly than in the tensor case. Figure 5.2 reports the convergence history of both methods for this problem. All matrices were preconditioned as described in section 4.1. TT rounding was performed with tolerance 10^{-9} and rank truncation 50. The same parameters were used for the truncation in MATRIX-LSQR. Truncation has a stronger negative impact in the matrix formulation, due to the fact that more information is lost after truncation. In the plot, we can appreciate the better accuracy achieved by the tensor method, in addition to the already mentioned lower memory requirements.

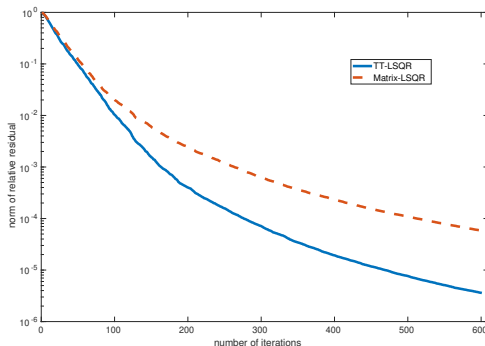


FIG. 5.2. Convergence history of TT-LSQR and MATRIX-LSQR for $n = 50$ for problems (5.1) and (5.3), resp., for the discretization of (5.2). Truncation threshold 10^{-9} , rank truncation 50.

6. Information retrieval, discrimination and classification in data mining. Documents such as scientific articles, newspaper reports, or email messages can be categorized according to different factors. Among the most commonly used ones are terms and keywords used within the documents themselves. In this framework, datasets are stored as matrices, where the rows correspond to the term dictionary, while the columns collect the distinct documents. The matrix entry (i, j) is binary if the term i is contained at least once in the document j , or a natural number if the number of times the term i occurs in the document j is collected.

In *information retrieval*, given a term-document matrix, the problem consists of finding a good representation of a new document (query) in terms of those in the

available dictionary. The problem can be cast as a least squares problem [14]. The largest components of the solution vector give an indication of the documents closest to the test query. Very often, the dictionary documents have already been clustered, so that they themselves are already collected in groups having similar features, such as a similar topic. In this case, it may be relevant to *aggregate* the new query as a member of one of the already separate clusters. In this case, since the clusters have common features, it may be appropriate to talk about *discriminant* analysis, rather than classification. Discriminant strategies have been used in multivariate statistics for a long time [19], and they allow one to distinguish among elemental groups by using features that are common within the group but different between groups.

On the other hand, classification is an important component of image processing, for which common/different features can be better identified than with text documents. Given a new image, corresponding for instance to a person’s face or to a specific class of objects (a car, a dog, etc), the procedure determines to which person or class of objects the new image belongs to. Each image is represented as a vector, a matrix or tensor of pixels. In the case of vectors, images are collected as adjacent columns of a matrix. Different matrices represent different persons or objects. Given a new image, comparing the corresponding vector with each different class using some distance measure allows one to classify the new image. Our formulation fits naturally this representation, and it will be used for one of the dataset in section 7.

A large number of classification methods, mostly for image processing, have been studied. They exploit different algorithmic devices, from the SVD to deep learning methods with matrix and tensor techniques, see, e.g., [5],[6],[16],[36] and their references. For both applications, discrimination and classification, we are interested in exploring how the special additive structure of the tensor formulation can provide a surplus value to these methodologies.

7. Discriminant analysis on clustered data. In the following we focus on the allocation of a new query, for already clustered data.

An interesting aspect in using a sum of tensor formulation in the LS problem for this type of data analysis is the flexibility in choosing the parameters ℓ , d , and m_i for $i = 1, \dots, d$. Fixed the number of modes d , if we want to use the same amount of memory, we can either choose to use more terms (larger ℓ) with fewer columns (smaller m_i), or choose to have more columns in each term (larger m_i) but with fewer terms (smaller ℓ). This has a multi-facet impact. Assuming $m = m_1 = \dots = m_d$, the memory required in the tensor representation throughout the iteration depends on m . Focusing on the TT-format, we have d core tensors with a memory requirement of the order of $\mathcal{O}(mr^2d)$, where r is the largest TT-rank of the solution tensor. The overall amount of memory required will be of the order of $\mathcal{O}(nmd\ell + mr^2d)$. If instead of ℓ terms we take only one term, to preserve the amount of information, the dimensions of \mathcal{X} should be increased to $m \times m \times \dots \times m$, where $\tilde{m} = m\ell$. Consequently, the new amount of memory required will be of the order of $\mathcal{O}(nmd + mr^2d)$. Using a bigger m not only increases the memory requirements but, more importantly, also increases the computational cost of each operation. Each iteration requires multiple applications of the tensor operator \mathcal{L} , leading to several truncation steps, thus affecting the final accuracy of the algorithm. We refer to Table 7.5 for an illustration of the effect of this selection on the method performance. Note that the selection of d is not left to the user, as it is mainly problem dependent. In all our experiments, TT rounding was performed only using the tolerance, 10^{-4} , and not the maximum rank dimension.

In the following we illustrate how the data are allocated to formulate the tensor

LS problem, and then we briefly describe the main properties of the datasets. Several numerical experiments follow.

7.1. Computational experiments: Preparing the setting. In this set of experiments we consider term-document matrices that have already been grouped according to their common features. Assume we have $d = 3$ groups, and let $\mathcal{A}_1, \mathcal{A}_2, \mathcal{A}_3$ be the corresponding matrices, each having \bar{m} columns. We then partition the group matrices so that we have ℓ blocks of size m for each group, so that $m\ell = \bar{m}$, that is

$$(7.1) \quad \mathcal{A}_j = [A_j^{(1)}, \dots, A_j^{(\ell)}], \quad A_j^{(i)} \in \mathbb{R}^{n \times m}, \quad j = 1, 2, 3.$$

We are thus ready to define the tensor operator

$$\mathbf{A} = \sum_{i=1}^{\ell} A_3^{(i)} \otimes A_2^{(i)} \otimes A_1^{(i)}.$$

Given the query vector f , consisting of the recurring keywords of a new document, we want to associate f with the closest group among the ones available, that is $\mathcal{A}_1, \mathcal{A}_2, \mathcal{A}_3$. To this end, we solve the least squares problem

$$\min_{\mathbf{x}} \|\mathbf{f} - \mathbf{A}\mathbf{x}\|_2$$

with the new method, where $\mathbf{f} = f \otimes f \otimes f$.

Once the structured least squares problem has been approximately solved, the classification of f consists of identifying the group of documents closest to f by using the solution \mathbf{x} . To this end, we investigate two criteria that exploit our new formulation.

Criterion 1²:

$$\hat{j} = \arg \max_{j=1,2,3} |(1 \otimes \overset{j}{f} \otimes 1) \left(\sum_{i=1}^{\ell} A_3^{(i)} \otimes A_2^{(i)} \otimes A_1^{(i)} \right) \mathbf{x}|, \quad (C1).$$

Criterion 2:

$$(7.2) \quad \hat{j} = \arg \max_{j=1,\dots,3} \|f^T U^{(j)}\|, \quad (C2)$$

where $U^{(j)}$ contains the left singular vectors of the unfolding in the mode j of $(\sum_{i=1}^{\ell} A_3^{(i)} \otimes A_2^{(i)} \otimes A_1^{(i)})\tilde{\mathbf{x}}$, and $\tilde{\mathbf{x}}$ is an approximation to the TT solution \mathbf{x} as described next. In the following we let $\mathbf{x} = \text{vec}(\mathcal{X})$. We first compute the TT-cores of the solution tensor, denoted $G^{(i)} \in \mathbb{R}^{r_{i-1} \times n_i \times r_i}$, then we compute their range basis using the SVD. Since all the TT-cores, except for the first and the last one, are 3-dimensional tensors, the SVD is performed with respect to the second mode, which coincides with the mode of the tensor we are working with,

$$(7.3) \quad [U^{(1)}, \sim] = \text{svd}(G^{(1)}), \quad [U^{(i)}, \sim] = \text{svd}(\hat{G}^{(i)}), \quad [U^{(d)}, \sim] = \text{svd}(G^{(d)T}),$$

where $\hat{G}^{(i)} \in \mathbb{R}^{n_i \times r_{i-1} \times r_i}$ denotes the unfolding along the second mode of the TT-core $G^{(i)} \in \mathbb{R}^{r_{i-1} \times n_i \times r_i}$. This procedure becomes expensive for a larger

²with $\overset{j}{f}$ we mean that f is positioned in either of the three Kronecker terms.

number of modes (i.e., high d) and for large TT-ranks. Instead of using the full solution tensor \mathcal{X} , the HOSVD of \mathcal{X} is computed and just the first column of each $U^{(i)}$ is stored. This means that $\mathcal{X}(i_1, \dots, i_d) \approx \tilde{\mathcal{X}}(i_1, \dots, i_d) := U^{(1)}(i_1, :)\cdots U^{(k)}(:, i_k, :)\cdots U^{(d)}(:, i_d)$, using the Tensor-Train notation. Then we apply the operator \mathcal{L} to $\tilde{\mathcal{X}}$, which will have TT-ranks equal to ℓ , the number of terms. The TT-cores of the tensor $\mathcal{L}(\tilde{\mathcal{X}})$ precisely correspond to the tensors $\tilde{U}^{(i)} \in \mathbb{R}^{\ell \times n_i \times \ell}$, used to classify the image f in the criterion (C2).

Criterion 2 is more expensive than Criterion 1, as it requires the SVD computation of the unfolded terms. If no truncation in \mathcal{X} were performed, we would expect (C2) to be more reliable as a discriminant criterion, as it may be viewed as a tensor generalization of the usual subspace projection criterion for data stored as matrices (see Criterion 4 below). On the other hand, the truncation may significantly weaken this strategy, with respect to (C1). Indeed, we noticed in our experiments that (C2) is not always more successful than (C1) in recognizing clustered data. For this reason, one could consider a combination of the two criteria to refine the classification. A more detailed analysis is left for future investigations.

We compare the quality of the success of the allocation with classical procedures in data mining that do not involve solving a tensor LS problem: a test for the allocation of queries in information retrieval, somewhat similar to simple query matching [4, section 3.1.2], and a test using range-oriented recognition [14, section 11.2].

Criterion 3: Partition $\mathbf{w} = \arg \min_{\mathbf{w}} \|\mathbf{f} - [\mathcal{A}_1, \mathcal{A}_2, \mathcal{A}_3]\mathbf{w}\|_2$ as $\mathbf{w} = [w_1; w_2; w_3]$, according to the partition of the coefficient matrix. For this matrix setting, and exploiting that the coefficient matrix has been normalized, we consider the following elementary query matching criterion:

$$\text{Doc } f \text{ belongs to Category } \hat{j} \text{ if } \hat{j} = \arg \max_j \|w_j\|_2 \quad (\text{C3}).$$

Criterion 4: Let \mathcal{U}_i , $i = 1, \dots, 3$ be the matrix whose 10 orthonormal columns span the leading portion of $\text{range}(\mathcal{A}_i)$. The matrix \mathcal{U}_i is obtained by a truncated SVD of \mathcal{A}_i to the first 10 singular triplets [14, Section 11.2]. Then

$$\text{Doc } f \text{ belongs to Category } \hat{j} \text{ if } \hat{j} = \arg \min_j \|f - \mathcal{U}_j \mathcal{U}_j^T f\| \quad (\text{C4}).$$

Criterion 3 requires solving a large matrix least squares problem, while Criterion 4 requires computing d truncated SVD of the corresponding matrices.

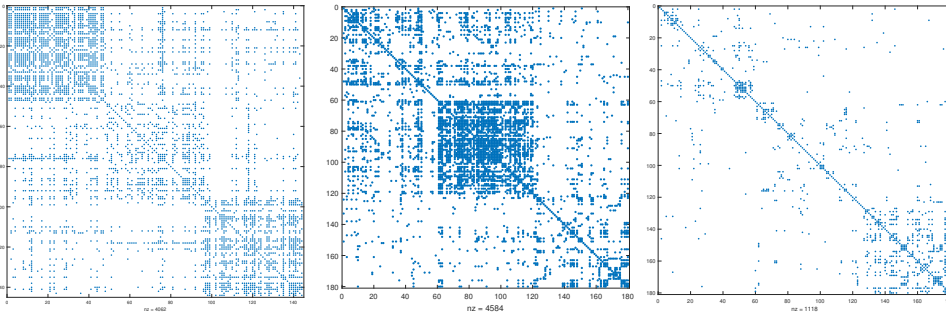


FIG. 7.1. Sparsity pattern of correlation matrices of \mathcal{A} in (7.1) with $m = 60$ for Reuters (left), Cranfield (middle), Medline (right); reported are elements above 0.15 in absolute value.

For our experimental investigation, we consider three term-document datasets available in popular repositories³:

- **Reuters21578**. This is a widely used collection of newswire articles from the Reuters financial newswire service, and it is an essential benchmark for text categorization research, with 8293 documents and 18933 keywords, giving a very sparse matrix with a total of 389455 nonzero entries. The documents are already assembled and indexed with categories, so that 65 clusters are already identified. In the following we will work with the three largest groups;
- **Cranfield**. This is a term-document matrix of scientific contexts on physics topics with 1,400 articles and a list of 4563 keywords, for a total of 81201 nonzero entries in the data matrix;
- **Medline**. This is a term-document matrix of medical contents with 1,033 articles and 5735 keywords, for a total of 51174 nonzero entries in the data matrix;

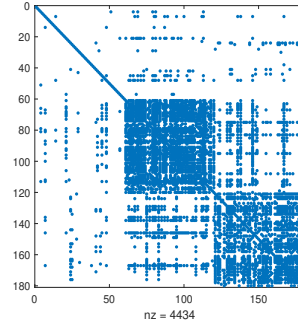


FIG. 7.2. Sparsity pattern of correlation matrix of A in (7.1) for FashionMNIST; with $m = 60$ reported are elements above 0.7 in absolute value.

Except for Reuters21578, the term-document datasets need to be divided into clusters, as described above. To this end, the K-means algorithm (available in Matlab) with three clusters was employed for each data set. By taking the computed clusters as categories, we have selected the first \bar{m} columns of each cluster as training sets, and the subsequent 20 columns as test set. Since the clustering is empirical, we do not expect exceptional success rates, although the results appear to be quite satisfactory in most cases.

We also consider a popular dataset of images:

- **Fashion_MNIST**⁴. This is a widely used dataset containing 70000 images of fashion products from Zalando. The images, stored as pixel vectors of length $784 = 28^2$, are divided into Training and Testing sets. As a preprocessing, we create two matrices of dimension $784 \times n_{\text{train}}$ and $784 \times n_{\text{test}}$ each, with $n_{\text{train}} = 60000$ and $n_{\text{test}} = 10000$. The products are already classified in 10 categories each representing a different type of clothing. In our experiments we consider only the three groups of footwear: sandals, sneakers and boots, in this order.

³These datasets are available at https://ir.dcs.gla.ac.uk/resources/test_collections/

⁴The dataset is available at <https://github.com/zalandoresearch/fashion-mnist>.

Category	\bar{m}	Tensor LS		Matrix LS	Proj norm
		Crit (C1)	Crit (C2)	method (C3)	(C4)
1	36	95	100	100	100
	48	95	100	100	100
	60	90	100	100	90
2	36	95	85	25	85
	48	85	95	10	85
	60	90	95	0	95
3	36	95	95	90	95
	48	95	95	85	85
	60	95	95	85	95

TABLE 7.1

Dataset Reuters. Percentage of success of classification for 20 test documents for different groups. $\ell = 6$, $d = 3$, $n = 18933$ for varying $\bar{m} = \ell m$.

Category	\bar{m}	Tensor LS		Matrix LS	Proj norm
		Crit (C1)	Crit (C2)	method (C3)	(C4)
1	36	55	65	10	75
	48	80	80	25	95
	60	65	95	40	85
2	36	100	100	100	95
	48	100	90	100	90
	60	95	85	100	80
3	36	85	95	10	95
	48	95	85	25	80
	60	75	85	10	70

TABLE 7.2

Dataset Cranfield. Percentage of success of classification for 20 test documents for different groups. $\ell = 6$, $d = 3$, $n = 4563$ for varying $\bar{m} = \ell m$.

Figure 7.1 shows the sparsity pattern of the correlation matrix associated with the term-document matrices, while Figure 7.1 shows the sparsity pattern relative to `FashionMNIST`. We can observe that some of the groups are strongly correlated, shown by a dense diagonal block (e.g., the second group of `Cranfield`). However, a good classification also depends on the sparsity of the off-diagonal blocks, which corresponds to low correlation between groups (e.g., the third group in `Cranfield`). We also notice the high sparsity of the `Medline` correlation matrix, particularly for all entries of the second group, predicting a possible low quality of a classification procedure. Similarly for the first group (sandals) of `Fashion_MNIST`.

7.2. Computational experiments: Testing the collocation strategy. The results of our analysis are reported in Tables 7.1-7.4, where the percentage of success in correctly classifying 20 test documents is reported. A fixed number of 10 iterations of TT-LSQR was used, as a very accurate solution is not the goal for this application. The TT truncation parameter was set to 10^{-4} . The tables show the performance as the total number $\bar{m} = \ell m$ of documents in the test group increases, with fixed $\ell = 6$. Since the test sample is small, the difference in success between 85% and 90% is given by a single extra failure, therefore a difference in 5% is considered not sufficiently large to make a case.

Category	\bar{m}	Tensor LS		Matrix LS	Proj norm
		Crit (C1)	Crit (C2)	method (C3)	(C4)
1	36	100	95	90	95
	48	95	85	75	90
	60	90	90	80	85
2	36	80	70	10	60
	48	55	55	10	25
	60	60	60	5	55
3	36	95	95	95	95
	48	95	95	100	95
	60	100	100	100	100

TABLE 7.3

Dataset Medline. Percentage of success of classification for 20 test documents for different groups. $\ell = 6$, $d = 3$, $n = 5736$ for varying $\bar{m} = \ell m$.

Category	\bar{m}	Tensor LS		Matrix LS	Proj norm
		Crit (C1)	Crit (C2)	method (C3)	(C4)
1	36	35	70	5	60
	48	65	75	0	75
	60	75	75	0	60
2	36	100	80	90	80
	48	100	85	95	100
	60	95	95	100	95
3	36	50	100	100	100
	48	30	95	70	95
	60	30	95	55	90

TABLE 7.4

Dataset Fashion_MNIST. Percentage of success of classification for 40 test documents for different groups. $\ell = 6$, $d = 3$, $n = 784$ for different values of $\bar{m} = \ell m$.

Table 7.1 shows that all test samples are quite well identified, and that tensor-based (C2) is the best criterion. On the other hand, the simple matrix LS criterion (C3) is quite unreliable, giving exceptionally bad rates for group 2. This performance is common to other datasets. The results for the other term-document tests lead to similar conclusions, with a general preference of criterion (C2) over (C1) for the tensor strategy. We recall that except for **Reuters**, the term-document groups were constructed by a clustering pre-processing, so that classification errors are more likely.

Table 7.4 shows that for the image dataset, the first group is the hardest to recognize. This behavior is justified by the low correlation of the first group, as shown in Figure 7.2. The low correlation in the first group can be attributed to the significant differences among the images. Nonetheless, the tensor strategy performs well, equipped with criterion (C2). Finally, we observe that in most cases the classification performance does not seem to over-depend on the value of $\bar{m} = \ell m$ for any of the strategy, while $\bar{m} = 60$ is often (but not always) the most favourable. As already mentioned, some of the differences may depend on the strength of the category cluster.

We would like to linger over the role of ℓ and m , that is the data distribution among the available terms in the coefficient sum of tensors. For the application problem considered, the m columns of each mode can be differently distributed among

ℓ	m	# iter (avg)	CPU time (secs, avg)	(C2)
3	20	*200	1277.3	60
6	10	35	257.3	80
12	5	18	190.4	85

TABLE 7.5

Dataset Medline. Performance of TT-LSQR over 20 test documents as ℓ and m vary and are such that $\bar{m} = \ell m = 60$. Stopping criterion on the normal equation relative residual with $\text{tol}=10^{-4}$, and 200 maximum iterations. (*) Only 10 test documents are considered, due to excessive computational costs.

the terms: m columns for each of the ℓ terms, so that $m \cdot \ell = \bar{m}$. For fixed $\bar{m} = 60$, Table 7.5 illustrates the significant benefit, in terms of CPU time, of keeping m low, and use more terms in the sum, without sacrificing classification success. The displayed results refer to the dataset **Medline**, after solving problem (1.1) to classify 20 documents from the first group, and reach a tolerance for the residual norm of the normal equation less than 10^{-4} . A maximum of 200 iterations was allowed. In addition to significantly lower CPU times, using a small value of m , that is thin matrices $A_j^{(i)}$, allows one to work with lower rank tensors throughout the TT-LSQR computation, making the iterations lighter. It is also interesting that convergence to the required residual norm tolerance is much faster for small m . These two properties lead to dramatically lower CPU times for smaller m .

7.3. Computational experiments with sketching. In Table 7.6 we report the performance of the sketched versus the unsketched tensor least squares problem, using a fixed number of iterations of TT-LSQR, equal to 10. Two of the datasets are considered. The percentage of successful classification is reported. For the first category, CPU times are also included; since times are very similar for the other categories, they are not reported in the table. We notice the drastic reduction of CPU time for the sketched problem, with in most cases an acceptable decrease in performance.

In spite of the convenient bound in (4.1), the sketched solution may significantly differ from the minimizer of the original problem. It was recognized in [27], [35] that the sketched solution \mathbf{x}_0 could be used as starting guess for an iterative procedure in terms of the original least squares problem. We have exploited this strategy in our setting as follows: we ran 30 iterations of the sketched problem at low cost, and then "regularized" the obtained solution by 2 iterations of TT-LSQR by solving the problem

$$(7.4) \quad \min_{\mathbf{z}} \|(\mathbf{f} - \mathcal{A}\mathbf{x}_0) - \mathcal{A}\mathbf{z}\|.$$

Our final solution will then be $\mathbf{x}_k = \mathbf{x}_0 + \mathbf{z}_k$. We explicitly remark that the idea of using \mathbf{x}_0 as starting guess suggested in [27], [35] requires that the sketched problem be solved exactly. To meet this constraint, we used 30 iterations of TT-LSQR on the sketched problem, and indeed running only 10 iterations was not sufficient to ignite the subsequent two iterations for (7.4). We remark that without truncation the starting residual $\mathbf{f} - \mathcal{A}\mathbf{x}_0$ has TT-rank larger than \mathbf{f} , therefore the two iterations of TT-LSQR may be expensive. The computational results of this strategy are reported in the two rightmost columns of Table 7.6 for each dataset. We see that the percentage of success often pays off the extra cost, compared with the purely sketched strategy. We believe this combined strategy deserved a deeper analysis.

Category	\bar{m}	MEDLINE			CRANFIELD		
		Tensor Sketched	Tensor	Tensor w/ StartSketch	Tensor Sketched	Tensor	Tensor w/ StartSketch
1	36	90 (0.7)	95 (38.9)	85 (13.9)	35 (0.7)	65 (27.2)	45 (11.2)
	48	80 (1.8)	85 (76.5)	85 (26.2)	85 (2.0)	80 (58.9)	70 (21.2)
	60	85 (4.3)	90 (121.9)	75 (50.9)	90 (4.4)	95 (96.5)	65 (33.3)
2	36	45	70	85	100	100	100
	48	45	55	55	95	90	100
	60	65	60	75	85	85	95
3	36	85	95	90	60	95	90
	48	85	95	90	95	85	70
	60	90	100	100	90	85	75

TABLE 7.6

Percentage of success of classification for 20 test documents for different categories, using criterion (C2). Comparison of Sketched TT-LSQR (10 its), TT-LSQR (10 its) and TT-LSQR (2 its) with the sketched solution (30 its) as starting guess. $\ell = 6$, $d = 3$, $n = 5736$ for varying \bar{m} . Sketching parameter $s = 2d\bar{m}$. In parenthesis is the average CPU time in secs - it is similar for all other categories.

8. Conclusions. We have proposed a tensorized version of the iterative method LSQR for solving tensor-oriented multiterm least squares. The implementation fully exploits available software packages for the Tensor-Train representation of the data, considerably lightening technical crucial steps such as rank truncation. We have focused our analysis on the use of tensor multiterm least squares in the context of allocating new document queries, and on the advantage of having a solver that can directly deal with this least squares formulation.

The obtained classification results are very promising and compare quite well with standard strategies, for instance in the case of the less exercised term-document datasets.

9. Acknowledgments. We would like to thank Davide Palitta for explanations on [7]. Both authors are members of the INdAM Research Group GNCS.

The work of VS was partially supported by the European Union - NextGenerationEU under the National Recovery and Resilience Plan (PNRR) - Mission 4 Education and research - Component 2 From research to business - Investment 1.1 Notice Prin 2022 - DD N. 104 of 2/2/2022, entitled “Low-rank Structures and Numerical Methods in Matrix and Tensor Computations and their Application”, code 20227PCCKZ – CUP J53D23003620006. The work of LP is funded by the European Union under the National Recovery and Resilience Plan (PNRR) - Mission 4 - Component 2 Investment 1.4 “Strengthening research structures and creation of “National R&D Champions” on some Key Enabling Technologies” DD N. 3138 of 12/16/2021 rectified with DD N. 3175 of 18/12/2021, code CN00000013 - CUP J33C22001170001.

Appendix. Tucker-LSQR. Given a tensor $\mathcal{X} \in \mathbb{R}^{n_1 \times \dots \times n_d}$ in Tucker format, that is

$$(9.1) \quad \mathcal{X} = \mathcal{C} \times_1 X_1 \times_2 X_2 \cdots \times_d X_d,$$

with $\mathcal{C} \in \mathbb{R}^{r_1 \times \dots \times r_d}$ and $X_i \in \mathbb{R}^{n_i \times r_i}$, an exact representation of \mathcal{X} is obtained for $r_i = n_i$. On the other hand, a Tucker tensor is low-rank if $r_i \ll n_i$ for all $i = 1, \dots, d$. When implementing the tensor LSQR with the Tucker format, the truncation step compresses the dimensions of the core tensor of the given tensor through the (truncated) Higher-Order SVD (HOSVD) developed in [12].

The Tucker structure can be deployed to sum up two tensors without explicitly building them. Let $\mathcal{A} = \mathcal{H} \times_1 U_1 \times_2 U_2 \cdots \times_d U_d$ and $\mathcal{B} = \mathcal{G} \times_1 V_1 \times_2 V_2 \cdots \times_d V_d$ have consistent dimensions, with $\mathcal{H} \in \mathbb{R}^{r_1 \times r_2 \times \cdots \times r_d}$ and $\mathcal{G} \in \mathbb{R}^{p_1 \times p_2 \times \cdots \times p_d}$. The sum tensor is $\mathcal{A} + \mathcal{B} = \mathcal{S} \times_1 W_1 \times_2 W_2 \cdots \times_d W_d$, where

$$W_i = [U_i, V_i],$$

and, setting $q_1 \times q_2 \times \cdots \times q_d$ where $q_i = r_i + p_i$,

$$\begin{aligned} \mathcal{S}(1 : r_1, 1 : r_2, \dots, 1 : r_d) &= \mathcal{H}, \\ \mathcal{S}(r_1 + 1 : q_1, r_2 + 1 : q_2, \dots, r_d + 1 : q_d) &= \mathcal{G}, \end{aligned}$$

which corresponds to the usual notation $\mathcal{S} = \text{blkdiag}(\mathcal{H}, \mathcal{G})$ (here in 3-mode tensor form); see Figure 9.1.

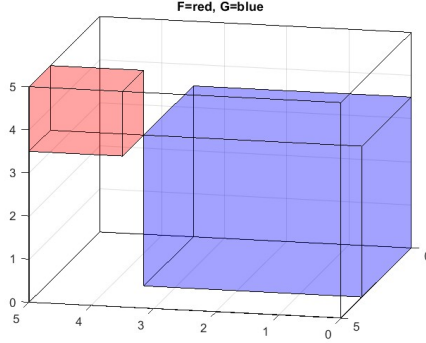


FIG. 9.1. Tensor core of the sum of two Tucker tensors, $\mathcal{S} = \text{blkdiag}(\mathcal{H}, \mathcal{G})$.

If no further action is taken, the core tensor dimensions of all constructed tensors increase within each iteration. Truncation is therefore necessary to control memory requirements. The matrix truncation strategy developed in [34] can be generalized to this setting.

Another advantage of the Tucker format follows from the following theorem.

THEOREM 9.1. ([18]) *For a given tensor $\mathcal{X} \in \mathbb{R}^{n_1 \times \cdots \times n_d}$ with independent Tucker decomposition $\mathcal{X} = \mathcal{C} \times_1 A^{(1)} \times_2 A^{(2)} \cdots \times_d A^{(d)}$, we have that*

$$(9.2) \quad \alpha \|\mathcal{C}\|_F \leq \|\mathcal{X}\|_F \leq \beta \|\mathcal{C}\|_F,$$

where $\beta = \|A^{(1)}\|_2 \|A^{(2)}\|_2 \cdots \|A^{(d)}\|_2$ and $\alpha = \beta / (\prod_{i=1}^d \kappa(A^{(i)}))$ with $\kappa(A^{(i)})$ being the condition number of the matrix $A^{(i)}$.

The result above shows that if for all i the matrix $A^{(i)}$ has orthonormal columns, the equality $\|\mathcal{X}\|_F = \|\mathcal{C}\|_F$ holds. More generally, the norm of the whole tensor can be monitored by that of the core.

REFERENCES

- [1] R. D. ALGARTE, *Tensor-based foundations of ordinary least squares and neural network regression models*, 2025.
- [2] A. H. BENTBIB, A. KHOUIA, AND H. SADOK, *The LSQR method for solving tensor least-squares problems*, *Electronic Transactions on Numerical Analysis*, 55 (2022), pp. 92–111.

- [3] M. BENZI AND M. TUMA, *A robust preconditioner with low memory requirements for large sparse least squares problems*, SIAM J. on Scientific Computing, 25 (2003), pp. 499–512.
- [4] M. W. BERRY AND M. BROWNE, *Understanding Searching Engines*, Software, Enviroments, and Tools, SIAM, Philadelphia, USA, 1999.
- [5] M. BOUSSÉ, N. VERVLIET, O. DEBALS, AND L. DE LATHAUWER, *Face recognition as a Kronecker product equation*, in IEEE 7th International Workshop on Computational Advances in Multi-Sensor Adaptive Processing (CAMSAP), Dec. 2017, pp. 1–5.
- [6] D. BRANDONI AND V. SIMONCINI, *Tensor-train decomposition for image recognition*, Calcolo, 57 (2020). article # 9.
- [7] A. BUCCI, D. PALITTA, AND L. ROBOL, *Randomized sketched TT-GMRES for linear systems with tensor structure*, Tech. Rep. 2409.09471, arXiv, 2024.
- [8] S.-Y. CHANG AND H.-C. WU, *Tensor-based least-squares solutions for multirelational signals and applications*, IEEE Transactions on Cybernetics, 54 (2024), pp. 2852–2865.
- [9] M. CHEN AND D. KRESSNER, *Recursive blocked algorithms for linear systems with Kronecker product structure*, Numerical Algorithms, 84 (2020), pp. 1199–1216.
- [10] C. F. DANTAS, J. E. COHEN, AND R. GRIBONVAL, *Learning tensor-structured dictionaries with application to hyperspectral image denoising*, in 27th European Signal Processing Conference, EUSIPCO 2019, A Coruña, Spain, September 2-6, 2019, IEEE, 2019, pp. 1–5.
- [11] C. F. DANTAS, M. N. DA COSTA, AND R. DA ROCHA LOPES, *Learning dictionaries as a sum of Kronecker products*, IEEE Signal Processing Letters, 24 (2017), pp. 559–563.
- [12] L. DE LATHAUWER, B. DE MOOR, AND J. VANDEWALLE, *A multilinear singular value decomposition*, SIAM J. on Matrix Analysis and Applications, 21 (2000), pp. 1253–1278.
- [13] S. V. DOLGOV AND D. V. SAVOSTYANOV, *Alternating minimal energy methods for linear systems in higher dimensions*, SIAM Journal on Scientific Computing, 36 (2014), pp. A2248–A2271.
- [14] L. ELDÉN, *Matrix methods in Data Mining and Pattern Recognition*, Fundamentals of Algorithms, SIAM, Philadelphia, USA, 2019. II ed.
- [15] W. HACKBUSCH, B. N. KHOROMSKIJ, AND E. E. TYRTYSHNIKOV, *Hierarchical Kronecker tensor-product approximations*, J. Numer. Math., 13 (2005), pp. 119–156.
- [16] N. HAO, M. E. KILMER, K. BRAMAN, AND R. C. HOOVER, *Facial recognition using tensor-tensor decompositions*, SIAM J. on Imaging Sciences, 6 (2013), pp. 437–463.
- [17] G. W. HOWELL AND M. BABOULIN, *LU preconditioning for overdetermined sparse least squares problems*, in Parallel Processing and Applied Mathematics, R. Wyrzykowski, E. Deelman, J. Dongarra, K. Karczewski, J. Kitowski, and K. Wiatr, eds., Cham, 2016, Springer International Publishing, pp. 128–137.
- [18] B. JIANG, F. YANG, AND S. ZHANG, *Tensor and its Tucker core: the invariance relationships*, Numerical Linear Algebra with Applications, 24 (2017), p. e2086.
- [19] R. A. JOHNSON AND D. W. WICHERN, *Applied multivariate statistical analysis*, Pearson Prentice Hall, NJ, 2007.
- [20] E. KERNFELD, M. KILMER, AND S. AERON, *Tensor-tensor products with invertible linear transforms*, Linear Algebra Appl., 485 (2015), pp. 545–570.
- [21] B. N. KHOROMSKIJ, *Tensors-structured numerical methods in scientific computing: survey on recent advances*, Chemometrics and Intelligent Laboratory systems, 110 (2012), pp. 1–19.
- [22] ———, *Tensor Numerical Methods in Scientific Computing*, De Gruyter, Berlin, Boston, 2018.
- [23] T. G. KOLDA AND B. W. BADER, *Tensor decompositions and applications*, SIAM Review, 51 (2009), pp. 455–500.
- [24] D. KRESSNER AND C. TOBLER, *Krylov subspace methods for linear systems with tensor product structure*, SIAM J. Matrix Anal. Appl., 31 (2010), pp. 1688–1714.
- [25] D. KRESSNER AND C. TOBLER, *Low-rank tensor Krylov subspace methods for parametrized linear systems*, SIAM. J. Matrix Anal. & Appl., 32 (2011), pp. 1288–1316.
- [26] P.-G. MARTINSSON AND J. A. TROPP, *Randomized numerical linear algebra: Foundations and algorithms*, Acta Numerica, 29 (2020), p. 403–572.
- [27] M. MEIER, Y. NAKATSUKASA, A. TOWNSEND, AND M. WEBB, *Are sketch-and-precondition least squares solvers numerically stable?*, SIAM J. on Matrix Analysis and Applications, 45 (2024), pp. 905–929.
- [28] I. OSELEDETS, *Tensor-train decomposition*, SIAM J. Scientific Computing, 33 (2011), pp. 2295–2317.
- [29] I. OSELEDETS, *TT-Toolbox*, 2025. <https://github.com/oseledets/TT-Toolbox>.
- [30] I. OSELEDETS AND E. TYRTYSHNIKOV, *TT-cross approximation for multidimensional arrays*, Linear Algebra and its Applications, 432 (2010), pp. 70–88.
- [31] I. V. OSELEDETS AND S. V. DOLGOV, *Solution of linear systems and matrix inversion in the TT-format*, SIAM Journal on Scientific Computing, 34 (2012), pp. A2718–A2739.
- [32] C. C. PAIGE AND M. A. SAUNDERS, *LSQR: An algorithm for sparse linear equations and sparse*

- least squares*, ACM Transactions on Mathematical Software (TOMS), 8 (1982), pp. 43–71.
- [33] D. PALITTA AND V. SIMONCINI, *Matrix-equation-based strategies for convection–diffusion equations*, BIT Numerical Mathematics, 56 (2016), pp. 751–776.
- [34] L. PICCININI AND V. SIMONCINI, *Truncated LSQR for Matrix Least Squares Problems*, To appear in Computational Optimization and Applications (COAP), (2025), pp. 1–22.
- [35] V. ROKHLIN AND M. TYGERT, *A fast randomized algorithm for overdetermined linear least-squares regression*, Proc. Natl. Acad. Sci. USA, 105 (2008), pp. 13212–13217.
- [36] N. A. SAPUTRA, L. S. RIZA, A. SETIAWAN, AND I. HAMIDAH, *A systematic review for classification and selection of deep learning methods*, Decision Analytics Journal, 12 (2024).
- [37] V. SIMONCINI, *Numerical solution of a class of third order tensor linear equations*, Bollettino UMI, 13 (2020), pp. 429–439.
- [38] D. P. WOODRUFF, *Sketching as a tool for numerical linear algebra*, Found. Trends Theor. Comput. Sci., 10 (2014), pp. 1–157.